INSTITUTE OF PHYSICS PUBLISHING NANOTECHNOLOGY
Nanotechnology **14** (2003) 204–211 PII: S0957-4484(03)53821-1

Plasma enhanced chemical vapour deposition carbon nanotubes/nanofibres—how uniform do they grow?

K B K Teo[1,7], S-B Lee[2], M Chhowalla[1], V Semet[3], Vu Thien Binh[3], O Groening[4], M Castignolles[5], A Loiseau[5], G Pirio[6], P Legagneux[6], D Pribat[6], D G Hasko[2], H Ahmed[2], G A J Amaratunga[1] and W I Milne[1]

[1] Department of Engineering, University of Cambridge, Trumpington Street, Cambridge CB2 1PZ, UK
[2] Microelectronics Research Centre, Cavendish Laboratory, University of Cambridge, Madingley Road, Cambridge CB3 OHE, UK
[3] Laboratoire d'Emission Electronique, DPM-CNRS, Université Lyon 1, Villeurbanne 69622, France
[4] Department of Physics, University of Fribourg, Pérolles, CH-1700 Fribourg, Switzerland
[5] Laboratoire d'Etude des Microstructures (LEM), ONERA-CNRS, BP72, 92322 Châtillon Cedex, France
[6] Thalès R&T France, Domaine de Corbeville, Orsay 91404, France

E-mail: kbkt2@eng.cam.ac.uk

Received 12 September 2002
Published 16 January 2003
Online at stacks.iop.org/Nano/14/204

Abstract
The ability to grow carbon nanotubes/nanofibres (CNs) with a high degree of uniformity is desirable in many applications. In this paper, the structural uniformity of CNs produced by plasma enhanced chemical vapour deposition is evaluated for field emission applications. When single isolated CNs were deposited using this technology, the structures exhibited remarkable uniformity in terms of diameter and height (standard deviations were 4.1 and 6.3% respectively of the average diameter and height). The lithographic conditions to achieve a high yield of single CNs are also discussed. Using the height and diameter uniformity statistics, we show that it is indeed possible to accurately predict the average field enhancement factor and the distribution of enhancement factors of the structures, which was confirmed by electrical emission measurements on individual CNs in an array.

1. Introduction

Since the report by Ren *et al* [1] that large areas of vertically aligned multiwall carbon nanotubes could be grown using plasma enhanced chemical vapour deposition (PECVD), there has been considerable interest in the use of this technique for the production of carbon nanotubes/nanofibres (CNs) as electron emission sources [2] in applications such as displays, microwave amplifiers and parallel electron beam lithography. Vertically aligned carbon nanotubes tend to possess better field emission properties than non-aligned nanotubes [3] and this is attributed to the large number of exposed tips of the aligned nanotube arrays which are sites responsible for high electric field enhancement. In the literature today, aligned CNs have been deposited from various plasma techniques such as hot filament PECVD [1], microwave PECVD [4], dc (glow discharge) PECVD [5, 6] and inductively coupled plasma PECVD [7]. It is clearly evident from these works that PECVD

[7] Author to whom any correspondence should be addressed.

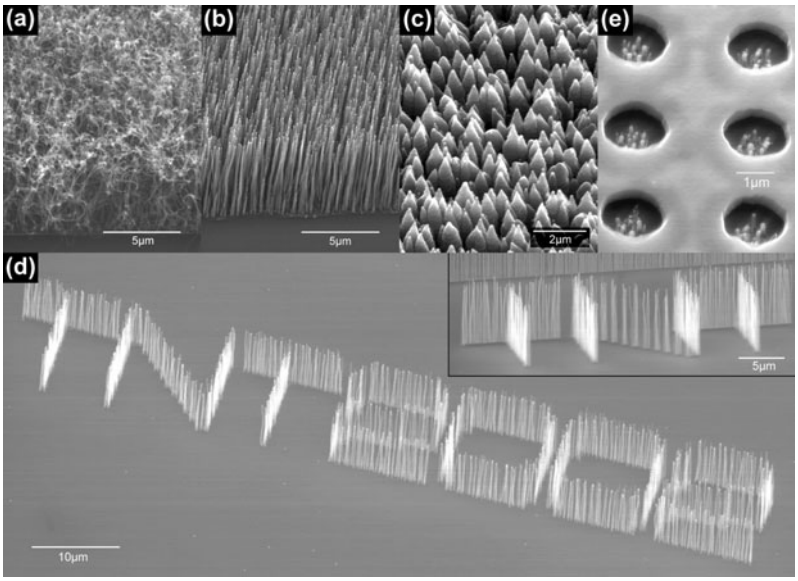

Figure 1. (a) Curly, non-aligned CNs deposited by thermal CVD. (b) Vertically aligned CNs deposited by PECVD. (c) Conical CNs deposited using a high (75%) C_2H_2 ratio in the gas flow. (d) Example of patterned growth of CNs. (e) Growth of vertically aligned CNs inside a gated field emission microcathode [13]. The tilt in these images were 45° except in the inset of (d) where a 75° tilt was used.

is a high yield and controllable method of producing vertically aligned CNs. In addition, for field emission applications, it is highly desirable that the emitters are spaced twice their height apart to avoid electric field screening [8] and the structural variation between emitters is as small as possible in order to achieve good emission uniformity. In general, the field enhancement factor of an isolated whisker-like CN structure is given by its height divided by the tip radius [9]. Recently, it was shown that isolated vertical CN structures can indeed be grown [5, 10, 11]; however, there are no data available on the uniformity of these PECVD-grown CN structures in terms of height, diameter, nucleation or electric field enhancement. This paper addresses these issues by evaluating the uniformity of CN structures achieved by PECVD and examining the electron emission uniformity from isolated CN structures.

2. Experiment and results

2.1. Growth of vertically aligned CNs by dc PECVD

The CN growth technique used in this paper is dc PECVD; this is perhaps the simplest type of plasma deposition to implement. The substrates used were n^+ doped Si ⟨100⟩ with a 8 nm diffusion barrier layer of SiO_2 or 20 nm barrier layer of conductive TiN [12]. In a conventional thermal chemical vapour deposition, the substrate, coated with a 3 nm film of Ni catalyst, was heated to 700 °C and then exposed to 40 sccm of C_2H_2 and 200 sccm of NH_3 gases at a partial pressure of 3.5 mbar. The thin film catalyst coalesced into nanoclusters at 700 °C which then seeded the growth of curly, spaghetti-like nanotubes as shown typically in figure 1(a). The dc PECVD technique is essentially the same except that the substrate was biased at −600 V to initate a dc glow discharge plasma. The electric field in the plasma sheath [6] causes the CNs to align vertically during growth as shown in figure 1(b). Moreover, the shape of the CNs could be varied from straight whisker-like to conical tip-like (figure 1(c)) by increasing the ratio of

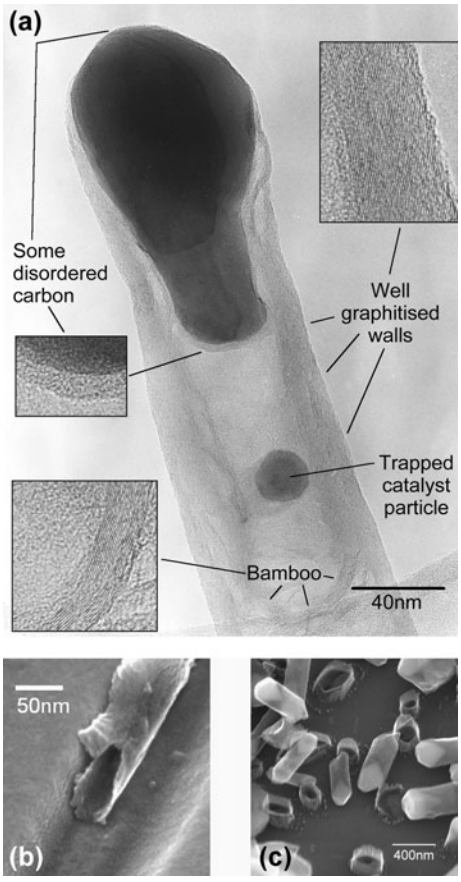

Figure 2. (a) Transmission electron micrograph of a dc PECVD CN. The insets shown are 2.5× magnified. Mechanically broken CNs are shown in (b) and (c), revealing their tubular, hollow structure.

C_2H_2 in the gas flow used [6, 13]. Patterned growth of CNs could be achieved by lithographically defining the Ni catalyst prior to growth. As seen in figure 1(d), the CN structures are

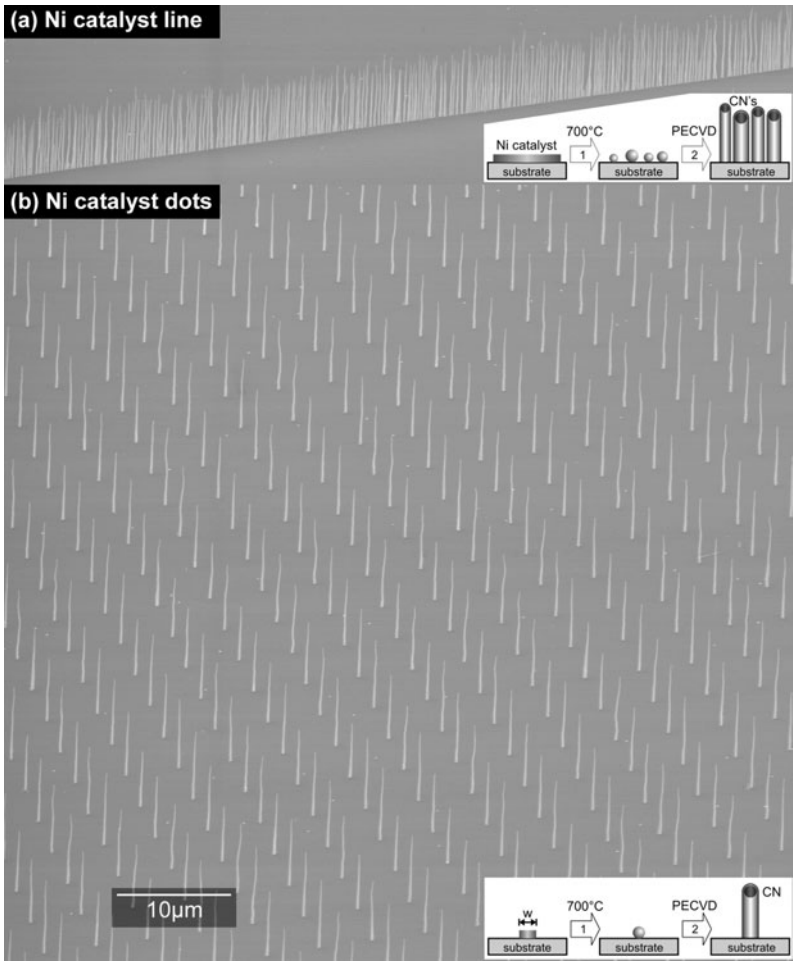

Figure 3. (a) CNs grown from a 100 nm wide, 7 nm thick Ni catalyst line. (b) CNs grown from 100 nm wide dots of 7 nm thick Ni catalyst. The tilt used was 55°.

really quite uniform. The height of the CN is controlled by the deposition time, which was 15 min for figures 1(a)–(d). Vertical CNs have also been successfully deposited directly inside gated microcathode arrays as shown in figure 1(e), and this microcathode exhibited a low turn-on voltage of 9–15 V and a peak emission current of 0.6 mA cm^{-2} at 40 V gate bias [14].

2.2. Structure of dc PECVD CNs

The transmission electron micrograph of a typical CN grown by dc PECVD is shown in figure 2(a). The Ni catalyst was observed at the tip of all CNs, which suggest that the deposition and catalyst support (i.e. substrate) conditions favour the tip-growth diffusion mechanism [15]. The CN contained 20–40 well crystallized graphene walls which were parallel to the axis of the CN. This suggests that these structures have excellent conductivity along their axis and indeed electrical conductivity measurements on individual PECVD CNs revealed that each exhibits a room temperature bulk resistivity of 10^{-6}–$10^{-5}\Omega$ m, comparable to multiwall carbon nanotubes by arc discharge [16], and have a maximum current carrying capability of 10^{7}–10^{8} A cm^{-2} [17]. Graphitic bamboo-like fringes were also observed along the length of the CN, as have been observed by others using PECVD [5, 18]. At the termination of growth when the catalyst cools down, it becomes covered by disordered carbon which is expelled due to the reduction in solubility of carbon in the catalyst as the temperature drops. Note from figures 2(b) and (c) that the structures produced by this process are in fact tubular and mostly hollow, even for extremely large diameter (300 nm) CNs.

2.3. Nucleation of multiple and single, isolated CNs

At this point, it is important to show the differences between the nucleation of multiple CNs from a 'large' catalyst film and the growth of a single isolated CN from a 'small' catalyst dot. To illustrate this, a 7 nm thick Ni film was patterned into a 100 nm wide line as shown in figure 3(a) and an array of 100 nm wide (w) square dots as shown in figure 3(b). It is immediately apparent that the catalyst line formed a single-file line of multiple CNs which had a significant variation in height (and diameter too, as will be shown later). In contrast, the array of catalyst dots produced relatively uniform CNs. The key difference here is that at 700 °C, the catalyst line coalesced to form multiple nanoclusters of different sizes which then catalysed the growth of 'uneven' CNs, as illustrated in the inset of figure 3(a). For the isolated 100 nm catalyst dots in the array, a single nanocluster of fixed volume/size was

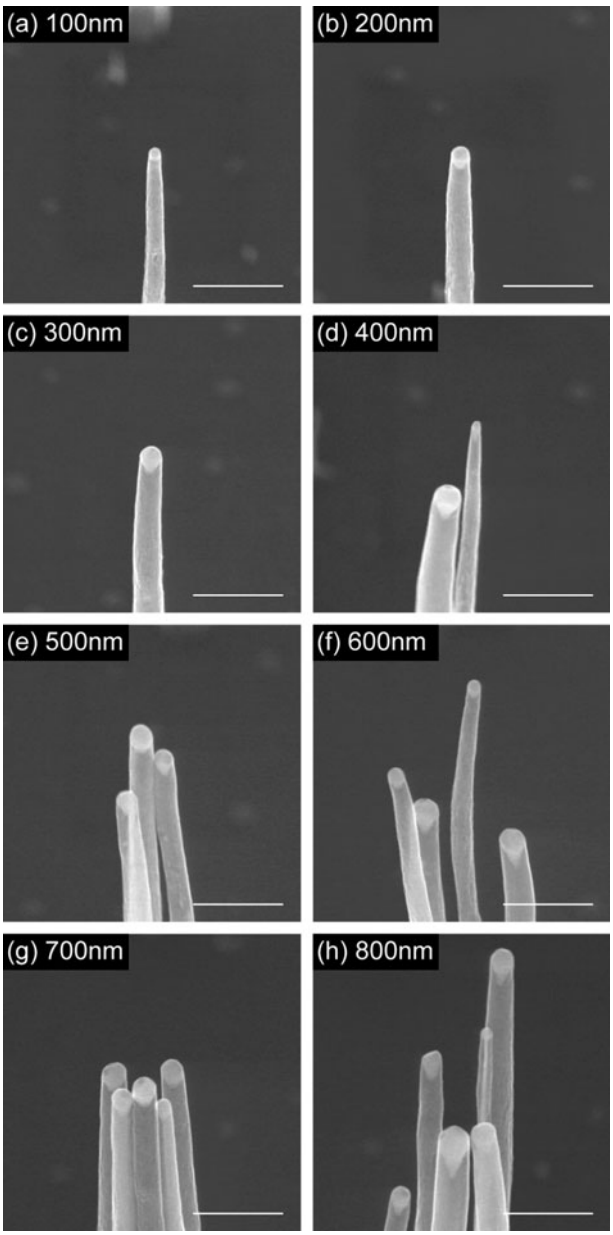

Figure 4. High resolution images of the heads of the CNs nucleated from Ni dots from (a) 100 to (h) 800 nm in width. The scale bar is 400 nm long and the sample tilt was 40°.

formed from each dot as shown in the inset of figure 3(b), which led to more identical CN deposition. And so, under what lithographic conditions can single CN growth be achieved and with what yield?

To answer this, arrays of square Ni dots were patterned using electron beam lithography in which the width of the catalyst (w in figure 3(b) inset) was varied from 100 to 800 nm. The Ni catalyst film thickness was fixed at 7 nm. The CNs were grown under typical conditions of C_2H_2:NH_3 flow of 40:200 sccm at a partial pressure of 3.5 mbar, 700 °C substrate temperature and −600 V substrate bias. Figure 4 shows the tips of typical CNs which were nucleated on these Ni dot arrays. It is evident that for Ni catalyst dots with sizes of 300 nm and below, single CNs per dot were nucleated. There were no instances when a catalyst dot did not nucleate at least one CN. It was observed that the base diameter of the CNs were slightly larger than the tip diameter, for example the 100 nm catalyst dots nucleated CNs whose tip diameter was 50 nm and base diameter was 200 nm. The larger base diameter was possibly due to sidewall deposition of carbon which caused the CNs to attain a slight conical shape [13]. However, the large height ($\sim$6 μm) of the CN structures meant that the half cone angle at the CN's apex was only $\sim$1°–2°, indicating that the structures were still overall whisker-like in shape.

As seen in figure 4, the critical size for the nucleation of single CNs was 300 nm, which is in good agreement with 350 nm found previously in an independent study [5]. However, this is a rather simplistic view because, when these CN arrays were examined with scrutiny, it was discovered that for both the 300 and 200 nm sized catalysts, there were still some instances of multiple (i.e. double) CNs from some catalyst dots (12% and 8% respectively). Thus, a statistical study was undertaken to determine the effect of the catalyst dot size on the number of CNs nucleated. Figure 5 shows histograms of the number of CNs nucleated per catalyst dot for sizes ranging from 100 to 800 nm derived from the observation of 500 catalyst dots in total. It was found that only at 100 nm were single CNs deterministically (100%) obtained.

The histograms were also fitted with normal distribution curves and there was a surprisingly good fit when multiple CNs were nucleated (i.e. $>$300 nm as in figures 5(d)–(h)). This confirms the stochastic/random nature of the formation of multiple nanoclusters which nucleate multiple CNs. The normal distribution fitting parameters, namely the average number of CNs and standard deviation, were plotted as a function of catalyst dot size in figure 6. Interestingly, beyond a 300 nm dot size, the average number of CNs was found to increase linearly with catalyst dot size (figure 6(a)) at a rate of approximately one nanotube per 91 nm increment in dot size. This shows that, to a certain extent, it is possible to control the number of CNs per catalyst dot by controlling the dot dimensions. However, note that the distribution in the number of CNs nucleated also increased with catalyst dot size, as shown in the standard deviation plot of figure 6(b). This shows that it is difficult to obtain the desired number of CNs per dot for large dot sizes. It is also apparent from figure 4 that when multiple CNs are nucleated, the CNs have a significant distribution in both diameter and height. For example, for the 800 nm catalyst dot size, there was a 4:1 ratio between the largest and smallest diameter CNs and $\sim$20% height variation (1.2 μm variation over 6 μm height) between the CNs. Overall, this indicates that the nucleation of multiple CNs from a large catalyst is a process with a significant degree of statistical spread in terms of number, height and diameter.

2.4. Height and tip diameter uniformity of single, isolated CNs

Thus, in order to achieve good structural uniformity, single isolated CNs must be grown—but how uniform are these isolated CNs? The tip diameter and height distribution of the arrays which contained individual CNs were investigated. The diameters of 150 single CNs, which were produced using 100–300 nm sized catalyst dots, were measured and the histograms showing their distributions are shown in figures 7(a)–(c). For

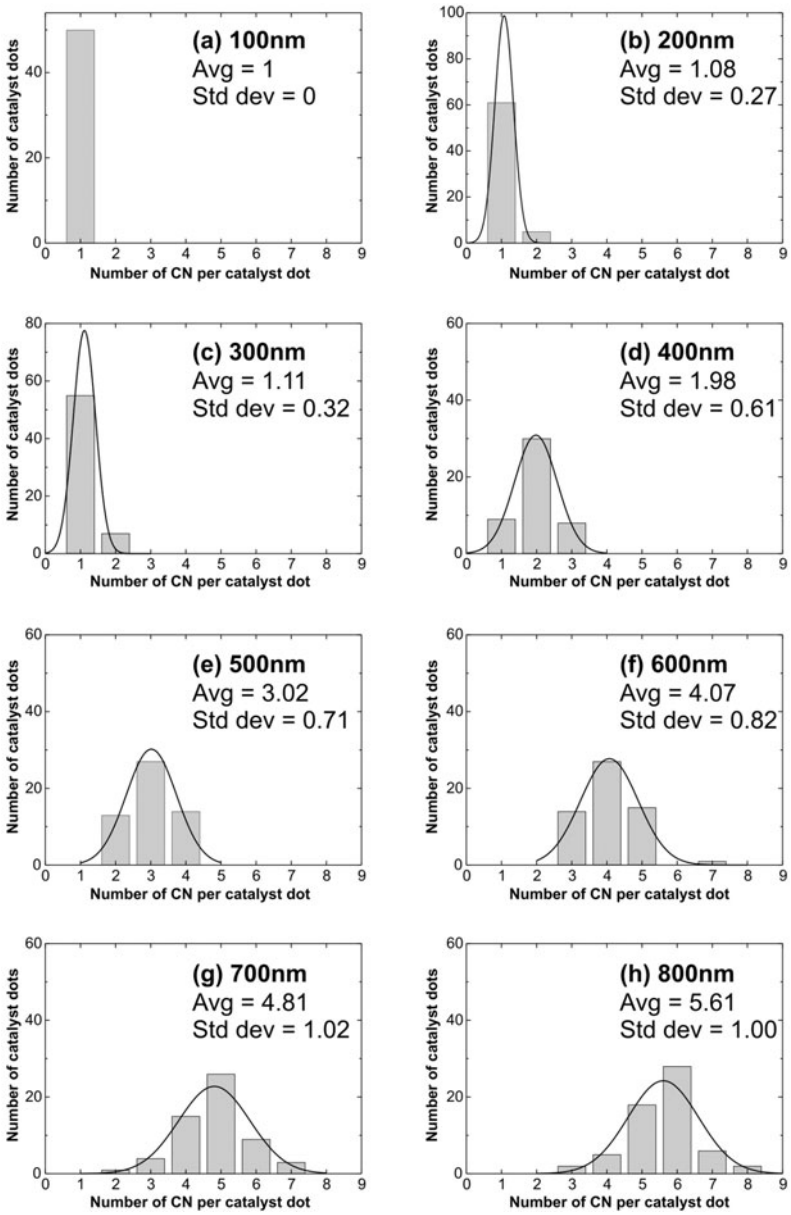

Figure 5. Histograms showing the occurrence of different number of CNs nucleated as the catalyst dot size was varied from (a) 100 to (h) 800 nm.

a particular dot size, a tight distribution in the CN diameters was observed and the standard deviation was 3.7–4.4% (mean 4.1%) of the average CN diameter from the three dot sizes. The average diameter was 49, 81 and 90 nm for the 100, 200 and 300 nm patterned Ni dots respectively. For comparison, figure 7(d) shows the distribution in diameters (60 CNs measured) from the 100 nm patterned catalyst line which nucleated multiple CNs. In this case, due to the 'random' coalescence of the catalyst, the standard deviation was much larger at 18% of the average nanotube diameter.

Note that in all cases the observed CN diameter was actually smaller than the catalyst dot size. This is because the catalyst forms a nanocluster of equal volume during growth. If it is assumed that the catalyst becomes a spherical nanocluster, the expected diameters of each CN after growth could be calculated by equating the volume of the patterned catalyst (e.g. for a 100 nm 'square' dot, 7 nm thick $= 100 \times 100 \times 7$ nm^3) with the volume of a sphere (i.e. $4/3\pi(\text{diameter}/2)^3$) due to conservation of the catalyst. The calculated nanotube diameters are thus 53, 85 and 111 nm for 100, 200 and 300 nm patterned catalyst dots. The observed diameters for the 100 nm patterned dots (49 nm) and 200 nm patterned dots (81 nm) do in fact correspond well to the calculated diameters. The observed diameters are actually slightly smaller than the calculated diameters because the nanocluster tends to elongate to form a droplet rather than maintain its spherical shape. For the 'large volume' 300 nm patterned catalyst, the catalyst clusters formed accentuated droplets which were 1.5×–2× longer than their diameter (see the large diameter CN of figure 4), thus producing smaller diameter CNs than predicted by the 'spherical' nanocluster assumption.

The distribution in heights for 160 CNs nucleated from 100 to 300 nm catalyst dots are shown in figures 8(a)–(c). A relatively tight distribution was observed and the

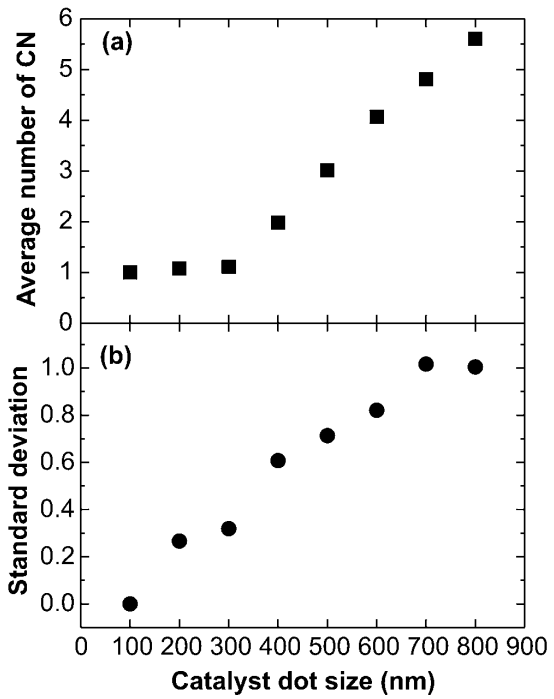

Figure 6. Plot of (a) the average number of CNs nucleated and (b) its standard deviation versus the catalyst dot size.

standard deviation was 5.7–6.8% (mean 6.3%) of the average height from the three dot sizes. For comparison, the height distribution of 60 nanotubes deposited from a 100 nm catalyst line, i.e. the multiple-nanotube nucleation case, is shown in figure 8(d). Again, the distribution is significantly wider (standard deviation 18% of average) because of the 'random' nature in which the patterned catalyst line broke up to form multiple nanoclusters which led to uneven growth.

Using the linear combination of errors approximation, it is now possible to estimate the standard deviation of the field enhancement factor (β = height/radius [9]) of single nanotubes to be 7.2–7.9% (mean 7.5%) of the average β. For the nanotubes nucleated from 100 nm dots, the average β was 240. Note that if the ratio distribution is assumed to be normal, it could be predicted statistically that average $\beta \pm 7.5\%$ would encompass 68% of the emitters, and $\beta \pm 15\%$ would cover 95% of the emitters.

2.5. Field emission uniformity of single isolated CNs

As the detailed field emission measurements on isolated CNs have been reported elsewhere [19], only a brief summary pertaining to the uniformity of the emission characteristics is provided here. The electron emission properties of individual isolated CNs, spaced 100 μm apart, were investigated using a scanning anode field emission system [19], similar to work performed by [20, 21]. As seen in figure 9(a), the Fowler–Nordheim characteristics of four adjacent emitters were very similar indeed. In fact, when these four emitters were subjected to a constant applied bias of 260 V from the anode, the emission currents extracted from each emitter were similar and in the microamp range per emitter (see the inset of figure 9(a)). The maximum emission currents observed from each CN were 10–20 μA before failure [19].

The CN uniformity statistics derived previously are now tested against observed enhancement factors from recent field emission I–V measurements. Scanning anode measurements [22] were performed on ten individual CNs

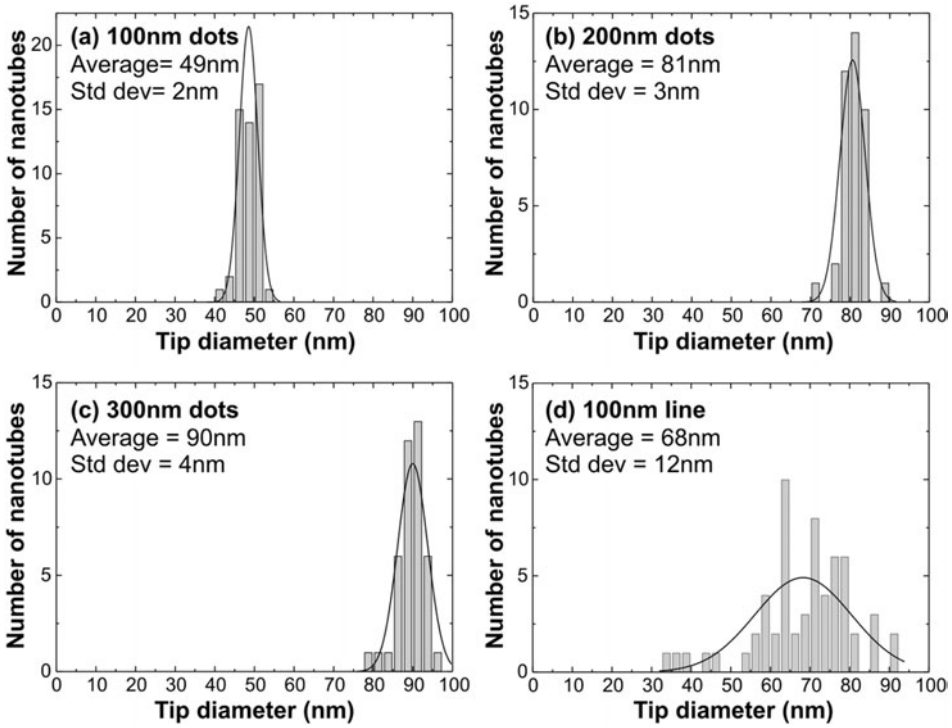

Figure 7. Distribution in CN diameters from (a) 100, (b) 200 and (c) 300 nm catalyst dot sizes. The distribution from multiple nanotubes nucleated from a 100 nm wide catalyst line is provided in (d).

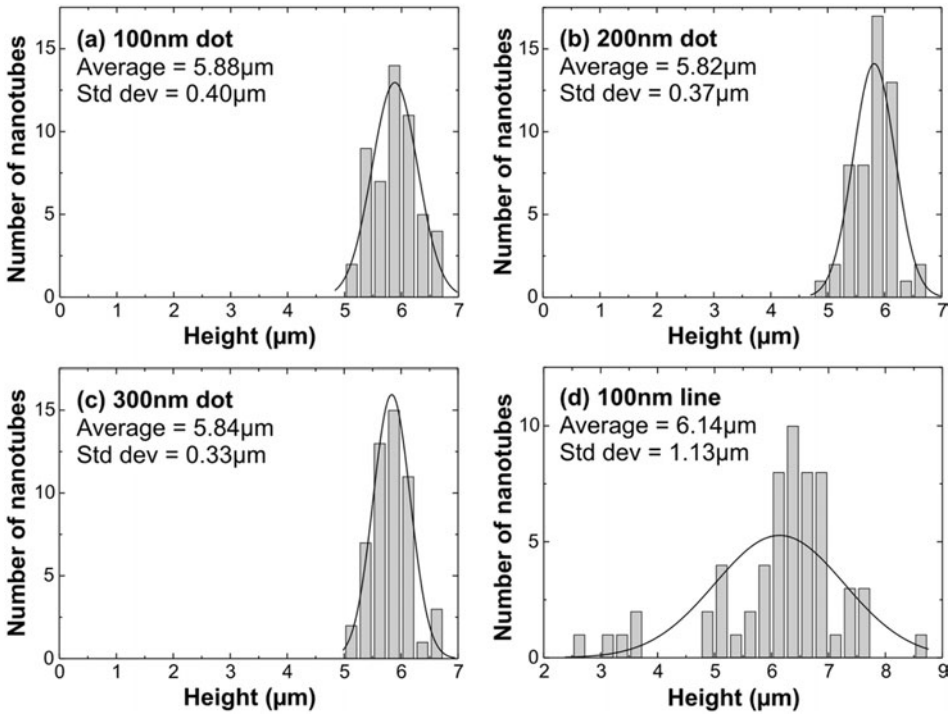

Figure 8. Distribution in CN heights for single CNs grown from (a) 100, (b) 200 and (c) 300 nm catalyst dots and (e) multiple nanotubes nucleated from a 100 nm wide catalyst line.

nucleated from 100 nm Ni dots spaced 25 μm apart. Assuming a typical work function of 4.9 eV [23], the enhancement factors, β, of these ten CNs were derived from electrical measurements (β_{FE}), and compared with the field enhancement factor was also derived directly from the geometry of these CN by scanning electron microscopy (β_{SEM}). The average height of the nanotubes was 5.83 μm and average radius was 24 nm, which are in good agreement with the dimensions of the nanotubes nucleated from 100 nm Ni dots in the previous section. The average β_{SEM} observed from these ten CNs was 249.

The first thing to note from figure 9(b) is that the average observed β_{SEM} of 249 corresponded well to the average electrically measured β_{FE} of 242, which was as expected from CNs nucleated from 100 nm dots ($\beta = 240$) in the previous section. This confirms that the emission mechanism from these CNs was indeed geometrically enhanced field electron emission. Additionally, this confirms the reproducibility of the deposition process since the 25 μm-spaced CN arrays measured here were fabricated in separate production runs to the 5 μm-spaced arrays used in the previous section.

Secondly, from figure 9(b), note that seven of the ten CN emitters had β_{FE} in the $\pm 7.5\%$ band, and nine of the ten emitters were within the $\pm 15\%$ band. This is in excellent agreement with the previous statistical prediction that 95% of the emitters would fall between $\beta \pm 15\%$, and 68% of the emitters would lie between $\beta \pm 7.5\%$. This experiment demonstrates the statistical reliability of the uniformity data.

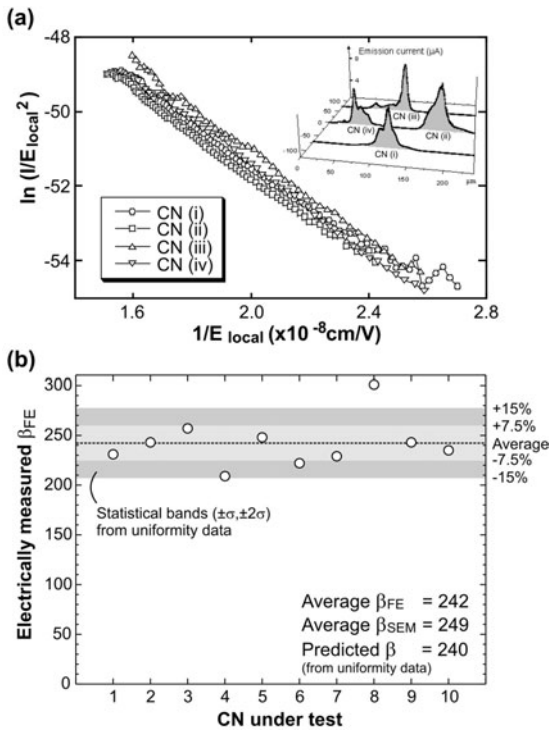

Figure 9. (a) Fowler–Nordheim plots and a current map at 260 V (inset) of four CNs in an array investigated using scanning anode field emission microscopy. (b) The field enhancement factors (β_{FE}) of ten CNs were obtained by emission measurements. The average β_{FE} and spread in the data are in agreement with the predicted statistical data obtained from the uniformity of the structures.

3. Conclusions

The nucleation and growth of multiple CNs from a 'large' patterned thin film catalyst is a random process which produces a significant distribution in the number of CNs nucleated, its diameter and its height. In contrast, the nucleation and

growth of a single, isolated CN is a controlled process which produced more uniform CNs in terms of diameter and height. In order to achieve high yield (>88%) of single CNs, the lithographic defining dimensions of the catalyst must be 300 nm or smaller, with 100 nm giving a 100% yield of single CNs. By statistically observing these single-CN arrays, the standard deviations in the diameter, height and geometrical enhancement (height/radius) of the single CNs were found to be 4.1, 6.3 and 7.5% of the averages respectively.

Moreover, electrical measurements have confirmed that the electron emission mechanism from these CNs is in fact geometrically enhanced field emission, and that these statistics pertaining to the CN's structural uniformity are in fact reliable in predicting the average and distribution of field enhancement factors. Having such a tight (and known) distribution of CN enhancement factors is desirable for field emission applications because it permits the design of efficient current ballasting systems to obtain homogeneous emission from a multitude of emitters. Furthermore, using this growth process, it is possible to tailor the geometry (diameter controlled by catalyst size, height controlled by deposition time) of the CN to obtain a desirable β for certain applications.

Acknowledgments

This work was funded by the European Commission through the IST-FET projects NANOLITH and CANVAD. One of the authors (KBKT) also acknowledges the support of the Association of Commonwealth Universities, the British Council and Christ's College Cambridge.

References

[1] Ren Z F, Huang Z P, Xu J W, Wang J H, Bush P, Siegal M P and Provencio P N 1998 *Science* **282** 1105

[2] See:
Bonard J-M, Kind H, Stockli T and Nilsson L 2001 *Solid State Electron.* **45** 893 for a review on carbon nanotube emitters

[3] Sveningsson M, Morjan R-E, Nerushev O A, Sato Y, Bäckström J, Campbell E E B and Rohmund F 2001 *Appl. Phys.* A **73** 409

[4] Bower C, Zhu W, Jin S and Zhou O 2000 *Appl. Phys. Lett.* **77** 830

[5] Merkulov V I, Lowndes D H, Wei Y Y, Eres G and Voelkl E 2000 *Appl. Phys. Lett.* **76** 3555

[6] Chhowalla M, Teo K B K, Ducati C, Rupesinghe N L, Amaratunga G A J, Ferrari A C, Roy D, Robertson J and Milne W I 2001 *J. Appl. Phys.* **90** 5308

[7] Delzeit L, McAninch I, Cruden B A, Hash D, Chen B, Han J and Meyyappan M 2002 *J. Appl. Phys.* **91** 6027

[8] Bonard J-M, Weiss N, Kind H, Stockli T, Forro L, Kern K and Chatelain A 2001 *Adv. Mater.* **13** 184
Nilsson L, Groening O, Emmenegger Ch, Kuettel O, Schaller E, Schlapbach L, Kind H, Bonard J M and Kern K 2000 *Appl. Phys. Lett.* **76** 2071
Gröning O, Küttel O M, Emmeneggar Ch, Gröning P and Schlapbach L 2000 *J. Vac. Sci. Technol.* B **18** 665

[9] Utsumi T 1991 *IEEE Trans. Electron Devices* **38** 2276

[10] Ren Z F, Huang Z P, Wang D Z, Wen J G, Xu J W, Wang J H, Calvet L E, Chen J, Klemic J F and Reed M A 1999 *Appl. Phys. Lett.* **75** 1086

[11] Teo K B K, Chhowalla M, Amaratunga G A J, Milne W I, Hasko D G, Pirio G, Legagneux P, Wyczisk F and Pribat D 2001 *Appl. Phys. Lett.* **79** 1534

[12] Rao A M, Jacques D, Haddon R C, Zhu W, Bower C and Jin S 2000 *Appl. Phys. Lett.* **76** 3813

[13] Merkulov V I, Guillorn M A, Lowndes D H, Simpson M L and Voekl E 2001 *Appl. Phys. Lett.* **79** 1178

[14] Pirio G, Legagneux P, Pribat D, Teo K B K, Chhowalla M, Amaratunga G A J and Milne W I 2001 *Nanotechnology* **13** 1

[15] Baker R T K 1989 *Carbon* **27** 315

[16] Forro L and Schnonenberger C 2001 *Carbon Nanotubes* ed M S Dresselhaus, G Dresselhaus and Ph Avouris (Berlin: Springer) pp 329–91

[17] Lee S-B, Teo K B K, Chhowalla M, Hasko D G, Amaratunga G A J, Milne W I and Ahmed H 2002 *Microelectron. Eng.* **61/62** 475

[18] Cui H, Zhou O and Stoner B R 2000 *J. Appl. Phys.* **88** 6072

[19] Semet V, Binh Vu Thien, Vincent P, Guillot D, Teo K B K, Chhowalla M, Amaratunga G A J, Milne W I, Legagneux P and Pribat D 2002 *Appl. Phys. Lett.* **81** 343

[20] Baylor L R, Merkulov V I, Ellis E D, Guillorn M A, Lowndes D H, Melechko A V, Simpson M L and Whealton J H 2002 *J. Appl. Phys.* **91** 4602

[21] Bonard J-M, Dean K A, Coll B F and Klinke C 2002 *Phys. Rev. Lett.* at press

[22] Nilsson L, Groening O, Kuettel O, Groening P and Schlapbach L 2002 *J. Vac. Sci. Technol.* B **20** 326

[23] Gröning O, Küttel O M, Emmeneggar Ch, Gröning P and Schlapbach L 2000 *J. Vac. Sci. Technol.* B **18** 665